Dental Materials Journal 2015; 34(3): 394–401

Fabrication of bone cement that fully transforms to carbonate apatite

Arief CAHYANTO[1,3], Michito MARUTA[2], Kanji TSURU[1], Shigeki MATSUYA[2] and Kunio ISHIKAWA[1]

[1] *Department of Biomaterials, Faculty of Dental Science, Kyushu University, 3-1-1 Maidashi, Higashi-ku, Fukuoka 812-8582, Japan*
[2] *Section of Bioengineering, Department of Dental Engineering, Fukuoka Dental College, 2-15-1 Tamura, Sawara-ku, Fukuoka 814-0193, Japan*
[3] *Department of Dental Materials Science and Technology, Faculty of Dentistry, Padjadjaran University, Jl. Raya Bandung Sumedang KM 21, Jatinangor 45363, Indonesia*
Corresponding author, Kanji TSURU; E-mail: tsuru@dent.kyushu-u.ac.jp

The objective of this study was to fabricate a type of bone cement that could fully transform to carbonate apatite (CO_3Ap) in physiological conditions. A combination of calcium carbonate ($CaCO_3$) and dicalcium phosphate anhydrous was chosen as the powder phase and mixed with one of three kinds of sodium phosphate solutions: NaH_2PO_4, Na_2HPO_4, or Na_3PO_4. The cement that fully transformed to CO_3Ap was fabricated using vaterite, instead of calcite, as a $CaCO_3$ source. Their stability in aqueous solutions was different, regardless of the type of sodium phosphate solution. Rate of transformation to CO_3Ap in descending order was Na_3PO_4>Na_2HPO_4>NaH_2PO_4. Transformation rate could be affected by the pH of solution. Results of this study showed that it was advantageous to use vaterite to fabricate CO_3Ap-forming cement.

Keywords: Bone cement, Carbonate apatite, Vaterite, Dicalcium phosphate anhydrous

INTRODUCTION

Apatite cement (AC) wields an advantage over calcium phosphate bone substitutes by virtue of its setting ability in physiological conditions. AC can set and harden in bone defects, then exhibit good osteoconductivity by transforming to apatite. Moreover, AC implantation in bone defects presents no gaps between AC and the existing bone due to the setting ability of AC. The absence of gaps further contributes to the higher osteoconductivity of AC[1)].

Another advantage possessed by AC lies in its ability to be replaced by bone. However, the replacement of AC by bone is still a matter under debate[2,3)]. Some researchers reported that AC was replaced by bone, while others claimed that it was only minimally replaced[4-10)]. We hypothesized that the replacement of AC by bone might be related to the carbonation of implanted AC in the body environment. The inorganic element of bone is CO_3Ap ($Ca_{10}(PO_4)_{6-x}(CO_3)_x(OH)_{2-x}$) which contains 4–8 weight% of carbonate in its apatitic structure[11)]. The carbonate content has a close relationship with osteoclastic resorption, in that CO_3Ap shows higher solubility in a weak acidic condition in Howship's lacuna produced by the osteoclasts[12)].

CO_3Ap granules fabricated by dissolution-precipitation reaction have shown osteoclastic bone resorption and new bone formation[13)]. This meant that for AC to be replaced by bone, the transformation of AC to CO_3Ap plays a pivotal role. On this premise, AC with high bone replacement ability could be developed if the starting materials of AC could transform to CO_3Ap after AC is implanted in the body. This also meant that in the fabrication of CO_3Ap-forming cement, the starting materials used should be in a semi-stable phase in order to yield the most thermodynamically stable apatite in the body environment.

The difference between AC and CO_3Ap-forming cement lies in the supply of CO_3^{2-} ions to the cement during reaction. For example, CO_3Ap-forming cement consisted of calcium carbonate ($CaCO_3$) and a possible candidate of dicalcium phosphate anhydrous (DCPA). When $CaCO_3$ and DCPA were mixed with an aqueous solution, $CaCO_3$ and DCPA dissolved and supplied Ca^{2+}, CO_3^{2-}, and PO_4^{3-} ions. The solution would be supersaturated with CO_3Ap as it is the most thermodynamically stable phase. Precipitates of CO_3Ap would form, then interlock each other to set and harden. Therefore, a possible starting material candidate in the fabrication of CO_3Ap-forming cement is a combination of $CaCO_3$ and DCPA.

Takagi *et al.*[14)] has reported that a combination of calcite, one of $CaCO_3$ crystals, and DCPA mixed with Na_2HPO_4 solution failed to fully transform to apatite. Moreover, mechanical strength was low (approximately 1–1.5 MPa)[14)]. The limited solubility of calcite might account for the failure to transform to apatite. Daitou *et al.*[15)] reported that calcite and DCPA (calcite-DCPA) could be fully transformed to CO_3Ap single phase *via* reaction with water but only at 70°C. This method is not viable for implantation in the body because of the high temperature. It is a fundamental requirement that AC must be applied and be able to set at body temperature.

Three kinds of polymorphs can be formed from $CaCO_3$: vaterite, aragonite, and calcite[16)]. Vaterite can be easily distinguished from among the $CaCO_3$ polymorphs: it has the highest solubility[17)]. Combes *et al.*[18)] reported that a combination of vaterite and brushite (V+Br) or aragonite, vaterite, and brushite (Ar+V+Br) mixed with 0.9% NaCl solution failed to be fully transformed to apatite. Moreover, these combinations took a longer time to set: 60 min for V+Br

Received May 14, 2014: Accepted Feb 5, 2015
doi:10.4012/dmj.2014-328 JOI JST.JSTAGE/dmj/2014-328

and 30 min for Ar+V+Br[18]. These combinations would not be useful for clinical application because of their long setting times. Deficiency of PO_4^{3-} ions during cement setting most probably accounted for the long setting times.

In the present study, CO_3Ap-forming cement was prepared using a combination of vaterite and DCPA (vaterite-DCPA) mixed with different kinds of sodium phosphate solutions. Properties of CO_3Ap-forming cement were then investigated in terms of setting and hardening time in physiological conditions and the ability to fully transform to CO_3Ap.

MATERIALS AND METHODS

Preparation of CO_3Ap-forming cement powders and liquids

Mixed vaterite-DCPA powder was employed as CO_3Ap-forming cement powder. DCPA powder (J.T. Baker Chemical, NJ, USA) was ground into particles of 0.4 µm size. Vaterite powder was prepared according to a previous report[19]. Briefly, 50 g of $Ca(OH)_2$ and 25 g of distilled water were added to 500 mL of methanol. CO_2 gas was blown for 120 min at a flow rate of 1 L/min into the suspension at 20°C. Gelation began when CO_2 gas was introduced into the suspension. After gelation, formed particles were collected by filtration and dried at 110°C. Vaterite powder and ground DCPA powder were mixed at a weight ratio of 40:60 to obtain the Vaterite-DCPA mixture powder.

To prepare calcite-DCPA mixture powder, commercial calcite powder (Wako Pure Chemical Industries, Osaka, Japan) was ground to obtain a particle size (0.3–0.5 µm) similar to that of vaterite powder (0.6–0.9 µm). Monosodium dihydrogen phosphate (NaH_2PO_4; pH 4.2), disodium hydrogen phosphate (Na_2HPO_4; pH 8.2), and trisodium phosphate (Na_3PO_4; pH 12.3) of 0.8 mol/L were used as cement liquid respectively.

Setting time measurement

CO_3Ap-forming cements were prepared at liquid-to-powder (L/P) ratios of 0.45, 0.55 and 0.65. Setting times of CO_3Ap-forming cements were measured according to the method set forth in ISO 1566 for dental zinc phosphate cements. In this method, a cement is considered to set when a 400-g weight loaded onto a Vicat needle with a tip diameter of 1.0 mm fails to make perceptible circular indentation at the surface of the cement. The standard requires the cement to be maintained at a temperature of 37°C and 100% relative humidity to simulate the clinical condition. In the present study, the specimen was placed on Teflon mold for setting time measurement. Mean setting time (n=3) was obtained, and the standard deviation was used as an evaluation of standard uncertainty.

Consistency evaluation

The consistency of CO_3Ap-forming cement paste was evaluated according to the method set forth in ISO 1566 for dental zinc phosphate cements. In the present study, consistency was evaluated using the diameter of the cement's spread area when 2 kg of glass plates was placed on 0.2 mL of the cement paste. Spread area was measured after a 3-min delay for L/P ratios of 0.45, 0.55, and 0.65. Three specimens were employed for consistency evaluation.

Structural analysis of crystal transformation to CO_3Ap

Set CO_3Ap-forming cement specimens of L/P ratio 0.45 were ground to obtain a fine powder for X-ray diffraction (XRD) analysis. XRD analysis was done using an X-ray diffractometer (D8 Advance, Bruker AXS, Karlsruhe, Germany) with CuKα radiation operated at 40 kV of tube voltage and 40 mA of tube current. Fine powder specimen was also used for Fourier Transform-Infrared (FT-IR) analysis. The KBr method was carried out for FT-IR analysis. Fine powder specimen and KBr at 1:200 ratio (approximately) was mixed well, and the compacted pellets were put in a stainless steel die. A spectrometer (FT/IR-6200, JASCO, Tokyo, Japan) using a spectral resolution of 4 cm^{-1} was employed to examine structural changes specifically CO_3^{2-} ion replacing/substituting PO_4^{3-} and/or OH^- ion.

Before performing measurements, a pellet holder which contained only a KBr pellet was measured as the background. Commercial HAp (HAP-200, Taihei Chemical Industrial, Osaka, Japan) was employed as a reference for both analyses.

Carbonate ion content

Carbon contained in specimens was determined by CHN coder (MT-6, Yanako Analytical Instruments Corp., Kyoto, Japan). Carbonate ion content in each specimen (n=5) was calculated from the amount of carbon contained in the specimen. Standard deviation was used as an evaluation of standard uncertainty.

Morphological analysis

The morphologies of the top surface and fractured surface of the specimen were analyzed using a scanning electron microscope (SEM; S-3400N, Hitachi High Technologies, Tokyo, Japan) at 15 kV accelerating voltage after gold-palladium coating using a magnetron sputtering device (MSP-1S, Vacuum Device Co., Ibaraki, Japan).

Mechanical strength measurement

The mechanical strength of specimens was assessed in terms of diametral tensile strength (DTS). Powder and liquid phases were mixed with a spatula at an L/P ratio of 0.45. The paste was packed into a stainless steel mold (ø 6 mm in diameter ×3 mm in height). Both ends of the mold were covered by glass slides and clamped by a metal clip. The molds were then placed in a plastic container with distilled water to maintain 100% relative humidity. The plastic container was put into an incubator and kept at 37°C up to 96 h. After specimens were removed from the molds, they were immersed in acetone for 3 min and then dried in an oven at 80°C for 3 h.

The diameter and height of each specimen were measured using a micrometer (MDC-25MU, Mitutoyo, Kanagawa, Japan). The specimens were crushed using a universal testing machine (AGS-J, Shimadzu, Kyoto, Japan) at a crosshead speed of 1 mm/min. Average DTS value was calculated from the DTS values of at least 10 specimens.

Porosity measurement

Specimens for porosity measurement were prepared using the same method as those for mechanical strength measurement. Porosity was calculated based on the bulk density of set CO_3Ap-forming cement, which in turn was calculated using its volume and weight. Specimen volume was calculated from the diameter and height of specimen, which were measured using a micrometer (MDC-25MU). Total porosity was calculated using the following formulae (1) and (2), as well as the theoretical density of B-type CO_3Ap (2.98 g/cm^3)[20]. Total porosity was calculated as the average value of at least 10 specimens.

$$\text{Relative density (\%)} = (\text{Bulk density})/(\text{Theoretical density}) \times 100 \quad (1)$$

$$\text{Porosity (\%)} = 100\% - \text{Relative density (\%)} \quad (2)$$

Statistical analysis

For the statistical analysis of data pertaining to consistency, porosity and mechanical strength, one-way factorial ANOVA with Fisher's LSD method as a *post hoc* test was performed using KaleidaGraph 4.1 (Synergy Software, PA, USA). Statistical significance level was set at $p<0.05$.

RESULTS

Table 1 shows the setting time comparison between CO_3Ap-forming cement consisting of vaterite and that consisting of calcite. When mixed with 0.8 mol/L of Na_2HPO_4, the setting time of cement consisting of vaterite-DCPA was shorter than that consisting of calcite-DCPA. The difference in setting time stemmed from the higher solubility of vaterite.

Comparison of crystal transformation to CO_3Ap as examined by XRD is shown in Figs. 1 and 2. In 72 h, the cement composed of vaterite was successfully transformed to pure CO_3Ap. For the cement composed of calcite, full transformation to pure CO_3Ap did not occur at 72 h and the starting materials still remained even after 240 h. This result revealed that vaterite was more effective than calcite as a starting material for CO_3Ap-forming cement. Therefore, we continued to investigate

Table 1 Setting time of CO_3Ap-forming cement consisting of vaterite-DCPA compared with that of calcite-DCPA, when mixed with 0.8 mol/L of Na_2HPO_4 solution in L/P ratio of 0.45 (n=3)

Liquid	Powder	Setting time (min)
Na_2HPO_4	Vaterite+DCPA	11.3±0.1
Na_2HPO_4	Calcite+DCPA	19.1±0.2

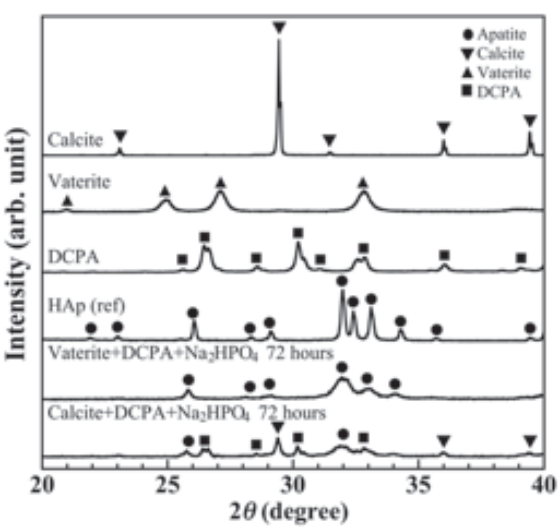

Fig. 1 Comparison of XRD patterns between CO_3Ap-forming cements consisting of calcite-DCPA and vaterite-DCPA mixed with Na_2HPO_4.

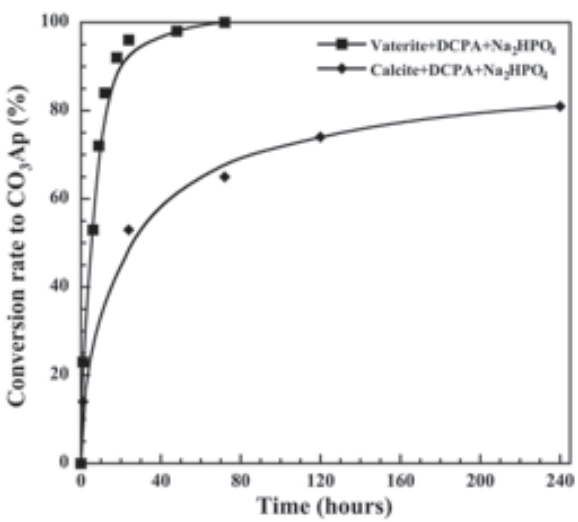

Fig. 2 Conversion rates of set CO_3Ap-forming cements consisting of ■ vaterite-DCPA and ◆ calcite-DCPA mixed with Na_2HPO_4.

the effects of different sodium phosphate solutions combining with CO_3Ap-forming cement which consisted of vaterite-DCPA.

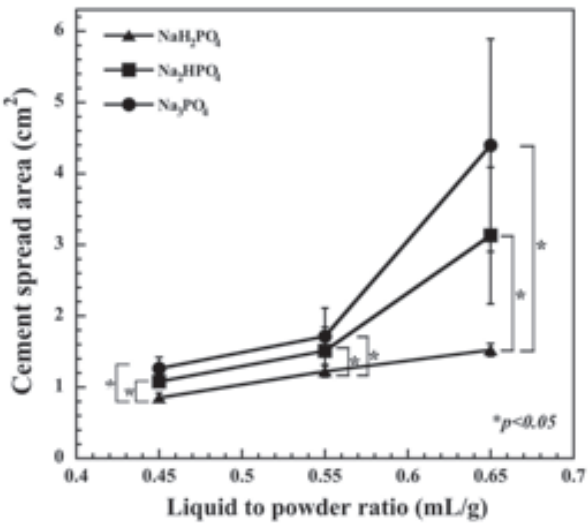

Fig. 3 Spread area of CO_3Ap-forming cement as a function of L/P ratio mixed with different sodium phosphate solutions: ─●─ Na_3PO_4, ─■─ Na_2HPO_4, ─▲─ NaH_2PO_4 (n=3). Error bars indicate the standard deviation.

Table 2 presents the setting times of CO_3Ap-forming cements prepared from different sodium phosphate solutions and at different L/P ratios. All cement pastes consisting of vaterite-DCPA could set within 20 min when 0.8 mol/L of sodium phosphate solution was used, regardless of the kind of sodium phosphate solution used. The setting times of all CO_3Ap-forming cements increased as L/P ratio increased, a tendency similar to those of gypsum and other dental cements. When distilled water was used as a cement liquid, the setting time became markedly longer because a longer time was required to reach supersaturation with respect to CO_3Ap.

Figure 3 presents the spread area of CO_3Ap-forming cement paste as a function of L/P ratio. The spread area of CO_3Ap-forming cement paste increased proportionally with increase in L/P ratio. This tendency was similar to those of gypsum and other dental cements. At each L/P ratio, different sodium phosphate solutions gave different results. There were no statistical differences between Na_3PO_4 and Na_2HPO_4, regardless of L/P ratio. In contrast, significant differences (p<0.05) were observed not only between NaH_2PO_4 and Na_3PO_4, but also between NaH_2PO_4 and Na_2HPO_4. Accordingly, the viscosity of cement paste mixed with NaH_2PO_4 was higher than those of Na_2HPO_4 and Na_3PO_4. The viscosity of cement paste might become higher when acidic solution was employed, although the reason remained

Table 2 Setting times of CO_3Ap-forming cements at different L/P ratios (n=3)

Liquid	Powder	Setting time (min)		
		L/P 0.45	L/P 0.55	L/P 0.65
NaH_2PO_4	Vaterite+DCPA	10.8±0.5	14.8±0.3	15.7±0.2
Na_2HPO_4	Vaterite+DCPA	11.3±0.1	15.4±0.4	16.7±0.5
Na_3PO_4	Vaterite+DCPA	16.6±0.2	18.0±0.6	19.6±0.4
Distilled water	Vaterite+DCPA	45.5±0.7	68.3±1.9	93.0±2.6

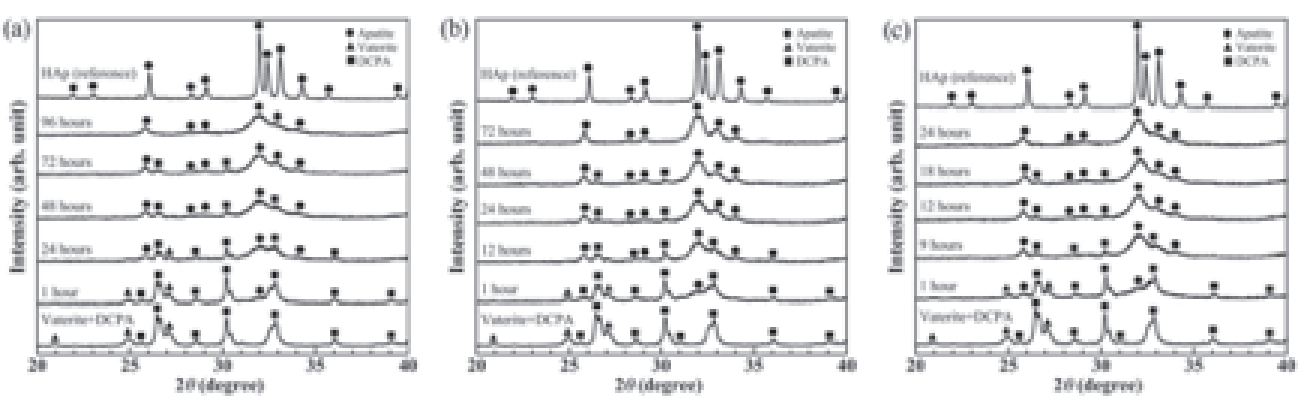

Fig. 4 XRD patterns of CO_3Ap-forming cements consisting of vaterite-DCPA and mixed with: (a) NaH_2PO_4, (b) Na_2HPO_4, and (c) Na_3PO_4.

to be clarified.

Figure 4 shows the before- and after-mixing XRD patterns of CO_3Ap-forming cements prepared from vaterite-DCPA and mixed with different sodium phosphate solutions. XRD pattern of commercial HAp is also shown as a reference. For all the sodium phosphate solutions used, a small peak assigned to apatite crystal was revealed within 1 h. Peak intensity gradually increased as treatment time increased. Based on these results, plotted curves showing the conversion of cement paste to CO_3Ap up to 96 h are shown in Fig. 5. Cement powder mixed with Na_3PO_4 solution showed the fastest transformation to CO_3Ap in 24 h. On the other hand, it took 72 h for Na_2HPO_4 solution and 96 h for NaH_2PO_4 solution. Therefore, conversion of set cement to CO_3Ap is in the descending order of Na_3PO_4>Na_2HPO_4>NaH_2PO_4.

Figure 6 shows the FT-IR spectra of CO_3Ap-forming cements prepared from vaterite-DCPA and mixed with different sodium phosphate solutions, using different treatment times. FT-IR spectrum of commercial HAp is also shown as a reference. For all the specimens, bands assigned to phosphate absorption were detected at 560–970 and 1,010–1,100 cm^{-1}. Similarly, additional bands around 872, 1,420 and 1,470 cm^{-1}, which were assigned to the absorption of CO_3^{2-} ions in its apatite structure, were detected[21]. A quantitative study of the carbonate content of CO_3Ap-forming cement prepared from different sodium phosphate solutions was carried out by CHN analysis, and the results are summarized in Table 3. The results were 11.4±0.4% for NaH_2PO_4, 12.3±0.7% for Na_2HPO_4, and 11.8±0.4% for Na_3PO_4.

Figure 7 shows the SEM images of the top surface and fractured surface of set CO_3Ap cements prepared from different sodium phosphate solutions. Results showed that the crystal sizes of set CO_3Ap cements prepared using different sodium phosphate solutions were almost similar. The CO_3Ap crystals interlocked each other to set and harden, regardless of the kind of sodium phosphate solution used. The fracture surfaces revealed a porous structure for set CO_3Ap cement. As shown in Fig. 8, the porosity values of set CO_3Ap cements were 58.1±0.9% for NaH_2PO_4, 57.3±1.8% for Na_2HPO_4, and 57.9±2.1% for Na_3PO_4. Among the three CO_3Ap cements, there were no statistical differences in porosity. In other words, set CO_3Ap cement had similar porosity irrespective of the kind of sodium phosphate solution used.

Figure 9 shows the DTS values of set CO_3Ap cements

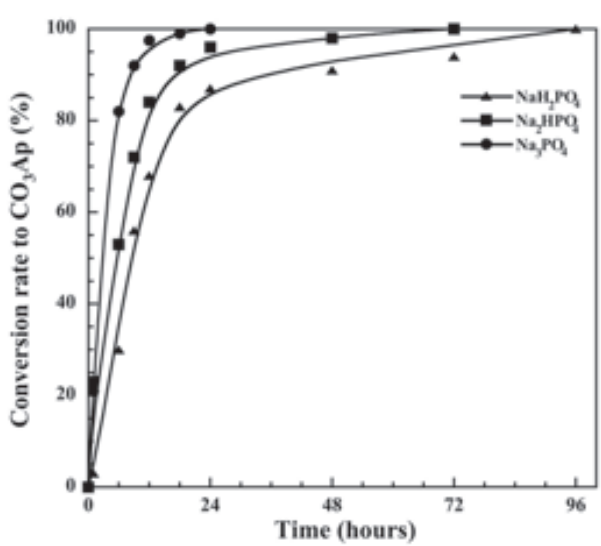

Fig. 5 Conversion rates of set CO_3Ap-forming cements as a function of time with different sodium phosphate solutions.

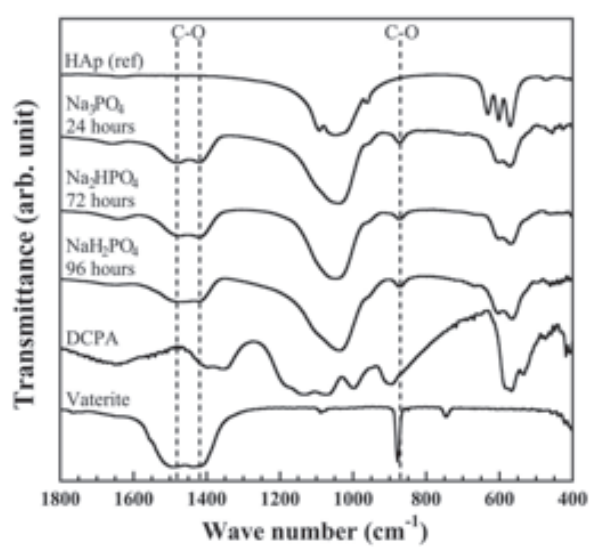

Fig. 6 FT-IR spectra of CO_3Ap-forming cements consisting of vaterite-DCPA and mixed with different sodium phosphate solutions after treatment for 24 h (Na_3PO_4), 72 h (Na_2HPO_4), and 96 h (NaH_2PO_4).

Table 3 Carbonate contents of CO_3Ap-forming cements after being treated for 24, 72 and 96 h and mixed with different sodium phosphate solutions at L/P ratio of 0.45 (n=5)

Liquid	Powder	Conversion to CO_3Ap (h)	CO_3^{2-} content (wt%)
NaH_2PO_4	Vaterite+DCPA	96	11.4±0.4
Na_2HPO_4	Vaterite+DCPA	72	12.3±0.7
Na_3PO_4	Vaterite+DCPA	24	11.8±0.4

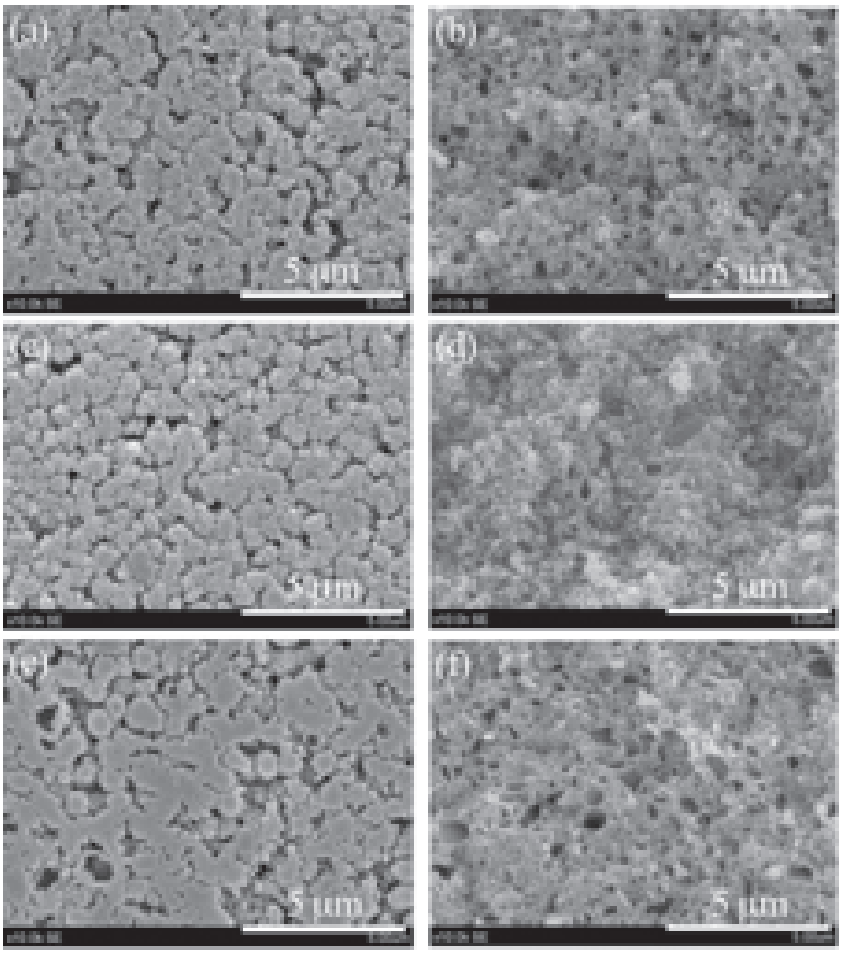

Fig. 7 SEM images of the outer surface (a,c,e) and the inner surface after fracture (b,d,f) of set CO_3Ap cements prepared from: (a,b) NaH_2PO_4, (c,d) Na_2HPO_4, and (e,f) Na_3PO_4.

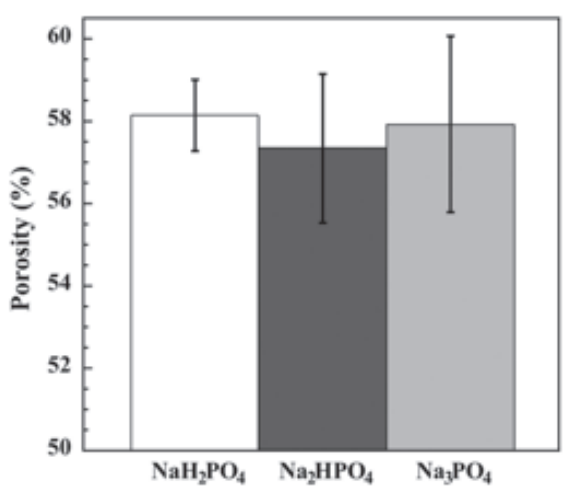

Fig. 8 Porosity of set CO_3Ap cements after treatment for 24 h (Na_3PO_4), 72 h (Na_2HPO_4), and 96 h (NaH_2PO_4). At least 10 specimens were measured for porosity. Error bars indicate the standard deviation.

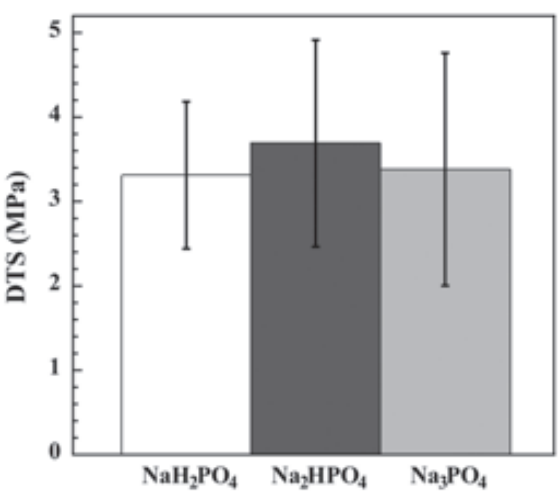

Fig. 9 DTS values of set CO_3Ap cements after treatment for 24 h (Na_3PO_4), 72 h (Na_2HPO_4), and 96 h (NaH_2PO_4).
At least 10 specimens were measured for DTS. Error bars indicate the standard deviation.

prepared from different sodium phosphate solutions. DTS values of set CO_3Ap cements were 3.3±0.9 MPa for NaH_2PO_4, 3.7±1.2 MPa for Na_2HPO_4, and 3.4±1.4 MPa for Na_3PO_4. Among the set CO_3Ap cements, there were no statistical differences in DTS value.

DISCUSSION

In the present study, a fast-setting cement which completely transformed to CO_3Ap was fabricated using vaterite instead of calcite as one of the starting materials (Table 1, Figs. 1 and 2). The CO_3Ap-forming cement which consisted of calcite-DCPA was not completely transformed to CO_3Ap even after 240 h (Fig. 2). This was caused by the limited solubility of calcite.

Setting and crystal transformation to CO_3Ap of this cement is based on dissolution-precipitation reaction. At the beginning, cement powders dissolved to supply Ca^{2+}, PO_4^{3-} and CO_3^{2-} ions. When the surrounding solution reached supersaturation with respect to CO_3Ap, CO_3Ap crystals were precipitated and entangled each other to form the set cement[22]. When vaterite was used instead of calcite, the higher solubility of vaterite than calcite[23,24] resulted in a faster dissolution of vaterite. The latter phenomenon then enabled the precipitation of CO_3Ap crystals to occur faster. Therefore, both setting reaction and crystal transformation to CO_3Ap occurred faster when vaterite was used instead of calcite.

For CO_3Ap-forming cement composed of vaterite-DCPA, the use of different sodium phosphate solutions gave different setting times and rates of crystal transformation to CO_3Ap. On setting time, the descending order beginning with the shortest setting time was NaH_2PO_4>Na_2HPO_4>Na_3PO_4 (Table 2). On crystal transformation to CO_3Ap, the descending order beginning with the fastest transformation was Na_3PO_4>Na_2HPO_4>NaH_2PO_4 (Figs. 4 and 5).

The setting reaction of apatite cements is similar to that of gypsum, in that the solubility difference between the starting material and the final product is a critical factor[25]. In a dissolution-precipitation reaction, precipitation cannot occur without prior dissolution of the starting material. When vaterite was used in an acidic condition, dissolution of the starting powders became accelerated[26]. With NaH_2PO_4 (pH 4.2), more bubble formation ($CaCO_3 \rightarrow CaO+CO_2 \uparrow$) was observed when compared with Na_2HPO_4 and Na_3PO_4. As the concentrations of Ca^{2+} and CO_3^{2-} ions quickly increased, it was easy to reach supersaturation with respect to apatite when NaH_2PO_4 was used. This was probably the reason why NaH_2PO_4 gave the shortest setting time. For apatite crystal transformation, an alkaline condition is more favorable since the most thermodynamically stable phase under alkaline condition is CO_3Ap. Therefore, Na_3PO_4 of pH 12.3 provided the fastest crystal transformation to CO_3Ap.

According to FT-IR analysis results (Fig. 6), set CO_3Ap cement obtained in this study corresponded to B-type CO_3Ap in that CO_3^{2-} ions in the apatitic structure replaced/substituted the PO_4^{3-} ions. LeGeros and Tung[27] reported that the solubility of CO_3Ap was affected by its carbonate content. Therefore, the CO_3Ap-forming cement obtained in this study was expected to have higher resorbability. The carbonate contents of CO_3Ap cements obtained in this study ranged between 11 and 12% (Table 3), which were higher than that in natural bone (4–8%).

Resorbability of cement is enhanced by a porous structure. In the present study, submicron-scale pores were observed in set CO_3Ap cements (Fig. 7). These pores were caused by generation of carbon dioxide gas during the setting reaction. Although the presence of pores in set CO_3Ap cement poses a negative effect to its mechanical strength, the DTS values of set CO_3Ap cements ranged between 3.3 and 3.7 MPa (Fig. 9), which still offered satisfactory strength for bone cement application. Although the porous structure of set CO_3Ap cement obtained in this study might not enhance the mechanical property, it would increase resorbability and improve cell attachment[28].

In vivo experiments using the CO_3Ap cement developed in this study have commenced. The cement could set even in the presence of body fluids or blood in rat tibial defects. Results of the *in vivo* study, which leveraged on the present study, would confirm whether this type of CO_3Ap-forming cement could enhance bioactivity and resorbability.

CONCLUSION

A cement which set quickly and which was completely transformed to CO_3Ap could be fabricated by using vaterite instead of calcite as carbonate ion source. The fast setting and quick transformation to pure CO_3Ap were caused by the higher solubility of vaterite when compared with calcite. A CO_3Ap-forming cement consisting of vaterite is expected to be an ideal bone replacement material.

ACKNOWLEDGMENTS

The first author is grateful to the Ministry of Education and Culture, Directorate of Higher Education (DIKTI), Republic of Indonesia for doctoral scholarship and to the Department of Dental Materials Science and Technology, Faculty of Dentistry, Padjadjaran University, Indonesia for supporting the doctoral study.

REFERENCES

1) Ishikawa K. Bioactive ceramics: cements. In: Ducheyne P, Healy KE, Hutmacher DW, Grainger DW, Kirkpatrick CJ, editors. Comprehensive biomaterials, 1st ed. Amsterdam: Elsevier; 2006. p. 268-282.
2) Ishikawa K. Calcium phosphate cement. In: Kokubo T, editor. Bioceramics and their clinical applications. New York: CRC Press; 2008. p. 438-463.
3) Cahyanto A, Tsuru K, Ishikawa K. Carbonate apatite formation during setting reaction of apatite cement. Proceedings of the 36th International Conference and Exposition on Advanced Ceramics and Composites; 2012 January 22–27; Daytona Beach, Florida, USA. Advances in

Bioceramics and Porous Ceramics V: Ceram Eng Sci Proc 2012; 33: p. 7-10.
4) Schneider G, Blechschmidt K, Linde D, Litschko P, Korbs T, Beleites E. Bone regeneration with glass ceramic implants and calcium phosphate cements in a rabbit cranial defect model. J Mater Sci Mater Med 2010; 21: 2853-2859.
5) Shindo ML, Constantino PD, Friedman CD, Chow LC. Facial skeletal augmentation using hydroxyapatite cement. Arch Otolaryngol Head Neck Surg 1993; 119: 185-190.
6) Constantino PD, Friedman CD, Jones K, Chow LC, Sisson GA. Experimental hydroxyapatite cement cranioplasty. Plast Reconstr Surg 1992; 90: 174-185.
7) Cancian DCJ, Vieira EH, Marcantonio RAC, Garcia Jr IR. Utilization of autogenous bone, bioactive glasses, and calcium phosphate cement in surgical mandibular bone defects in *Cebus apella* monkeys. Int J Oral Maxillofac Implants 2004; 19: 73-79.
8) Gosain AK, Riordan PA, Song L, Amarante MT, Kalantarian B, Nagy PG, Wilson CR, Toth JM, McIntyre BL. A 1-year study of osteoinduction in hydroxyapatite-derived biomaterials in an adult sheep model: part II. Bioengineering implants to optimize bone replacement in reconstruction of cranial defects. Plast Reconstr Surg 2004; 114: 1155-1163.
9) Friedman CD, Costantino PD, Takagi S, Chow LC. BoneSource™ hydroxyapatite cement: a novel biomaterial for craniofacial skeletal tissue engineering and reconstruction. J Biomed Mater Res 1998; 43: 428-432.
10) Miyamoto Y, Ishikawa K, Takechi M, Toh T, Yoshida Y, Nagayama M, Kon M, Asaoka K. Tissue response to fast-setting calcium phosphate cement in bone. J Biomed Mater Res 1997; 37: 457-464.
11) LeGeros RZ. Calcium phosphates in oral biology and medicine. Monogr Oral Sci 1991; 15: 1-201.
12) Leewenburgh S, Layrolle P, Barrère F, de Bruijn J, Schoonman J, van Blitterswijk CA, de Groot K. Osteoclastic resorption of biomimetic calcium phosphate coatings *in vitro*. J Biomed Mater Res 2001; 56: 208-215.
13) Ishikawa K. Bone substitute fabrication based on dissolution-precipitation reactions. Materials 2010; 3: 1138-1155.
14) Takagi S, Chow LC, Ishikawa K. Formation of hydroxyapatite in new calcium phosphate cements. Biomaterials 1998; 19: 1593-1599.
15) Daitou F, Maruta M, Kawachi G, Tsuru K, Matsuya S, Terada Y, Ishikawa K. Fabrication of carbonate apatite block based on internal dissolution-precipitation reaction of dicalcium phosphate and calcium carbonate. Dent Mater J 2010; 29: 303-308.
16) De Leeuw NH, Parker SC. Surface structure and morphology of calcium carbonate polymorphs calcite, aragonite, and vaterite: an atomistic approach. J Phys Chem B 1998; 102: 2914-2922.
17) Plummer LN, Busenberg E. The solubilities of calcite, aragonite and vaterite in CO_2-H_2O solutions 0 and 90°C, and an evaluation of the aqueous model for the system $CaCO_3$-CO_2-H_2O. Geochemica et Cosmochimica Acta 1982; 46: 1011-1040.
18) Combes C, Bareille R, Rey C. Calcium carbonate-calcium phosphate mixed cement compositions for bone reconstruction. J Biomed Mater Res 2006; 79A: 318-328.
19) Maeda H, Maquet V, Chen QZ, Kasuga T, Jawad H, Boccaccini AR. Bioactive coatings by vaterite deposition on polymer substrates of different composition and morphology. Mat Sci Eng C 2007; 27: 741-745.
20) Landi E, Tampieri A, Celotti G, Vichi L, Sandri M. Influence of synthesis and sintering parameters on the characteristics of carbonate apatite. Biomaterials 2004; 25: 1763-1770.
21) Lafon JP, Champion E, Bernache-Assollant D. Processing of AB-type carbonated hydroxyapatite $Ca_{10-x}(PO_4)_{6-x}(CO_3)_x(OH)_{2-x-2y}(CO_3)_y$ ceramics with controlled composition. J Eur Ceram Soc 2008; 28: 139-147.
22) Ishikawa K, Matsuya S. Bioceramics. In: Milne I, Ritchie RO, Karihaloo B, editors. Comprehensive structural integrity, Vol. 9. Oxford: Elsevier; 2003. p. 169-214.
23) De Visscher A, Vanderdeelen J. Estimation of the solubility constant of calcite, aragonite, and vaterite at 25°C based on primary data using the pitzer ion interaction approach. Monatshefte für Chemie 2003; 134: 769-775.
24) Cahyanto A, Maruta M, Tsuru K, Matsuya S, Ishikawa K. Basic properties of carbonate apatite cement consisting of vaterite and dicalcium phosphate anhydrous. Key Eng Mater 2013; 529-530: 192-196.
25) Nomura S, Tsuru K, Maruta M, Matsuya S, Takahashi I, Ishikawa K. Fabrication of carbonate apatite blocks from set gypsum based on dissolution-precipitation reaction in phosphate-carbonate mixed solution. Dent Mater J 2014; 33: 166-172.
26) Gal JY, Bollinger JC, Tolosa H, Gache N. Calcium carbonate solubility: a reappraisal of scale formation and inhibition. Talanta 1996; 43: 1497-1509.
27) LeGeros RZ, Tung MS. Chemical stability of carbonate- and fluoride-containing apatites. Caries Res 1983; 17: 419-429.
28) Del Valle, Miño N, Muñoz F, González A, Planell JA, Ginebra MP. *In vivo* evaluation of an injectable macroporous calcium phosphate cement. J Mater Sci Mater Med 2007; 18: 353-361.